Mathematical model for characterizing noise transmission into finite cylindrical structures

Deyu Li and Jeffrey S. Vipperman[⊥]

Department of Mechanical Engineering

University of Pittsburgh

Pittsburgh, Pennsylvania 15261

[⊥]Corresponding author

Jeffrey S. Vipperman

Department of Mechanical Engineering

648 Benedum Hall

3700 O'Hara Street

University of Pittsburgh

Pittsburgh, Pennsylvania 15261

(412) 624-1643 (voice)

(412) 624-4846 (fax)

PACS number: 43.40.Ey, 43.40.Fz, 43.20Fn, 43.20.Ks

Running Headline: Noise Transmission Model for Finite Cylinders

This work presents a theoretical study of the sound transmission into a finite cylinder under coupled structural and acoustic vibration. Particular attention of this study is focused on evaluating a dimensionless quantity, "noise reduction," for characterizing noise transmission into a small cylindrical enclosure. An analytical expression of the exterior sound pressure resulting from an oblique plane wave impinging upon the cylindrical shell is first presented, which is approximated from the exterior sound pressure for an infinite cylindrical structure. Next, the analytical solution of the interior sound pressure is computed using modal-interaction theory for the coupled structural acoustic system. These results are then used to derive the analytical formula for the noise reduction (NR). Finally, the model is used to predict and characterize the sound transmission into a ChamberCore cylindrical structure, and the results are compared with experimental data. The effects of incidence angle and internal acoustic damping are also presented.

I. INTRODUCTION

Thin composite cylindrical structures play an important role in aerospace industry due to their lighter weight, higher strength, and larger stiffness when compared to their aluminum or steel counterparts.[1-5] Unfortunately the noise transmission into such cylindrical enclosures is worse because of the light nature of composites.[1-4] As part of a noise transmission study for composite structures, a theoretical model to characterize the noise transmission into finite thin-wall cylindrical structures is developed.[1]

The problem of sound transmission through infinite, homogeneous, isotropic thin cylindrical structures has been investigated in some detail by several researchers. Tang *et al*. studied an infinite cylindrical sandwich shell with honeycomb core.[6,7] A simplified analysis of sound transmission through a finite, closed cylindrical shell was first proposed by White,[8] while the sound radiation into the acoustic cavity enclosed by a finite cylindrical shell with end plates was studied by Cheng.[9] Tso and Hansen derived a coupling loss factor for a cylindrical/plate structure using statistical energy analysis,[10] their method, however, does not work well at low frequencies and further could not show the effects on sound transmission of the cavity resonances. Koval first presented a mathematical "noise reduction" (*NR*) model to account for the effects of cavity resonances on sound transmission into a thin cylindrical shell.[11] In his model, the axial modes of the cylindrical cavity are neglected, because both the cylindrical shell and the internal acoustic cavity are considered to be infinite in length. Actually, both structural and acoustic axial modes of a finite cylindrical structure are experimentally found to be very important modes for noise control in low frequencies.[1,4,12] Gardonio, Ferguson and Fahy presented an expression of *NR* to characterize unit amplitude external incident sound transmission through a finite cylindrical shell.[13] From the equation of definition it is seen that the *NR* is defined based on the one proposed by Koval. However, the definition has some differences with Koval's *NR*. In Gardonio's *NR*, the external sound pressure is considered to equate the incident, unit amplitude sound, and they ignore the effects of scattering sound from the cylindrical shell on the external sound field. Estève and Johnson included axial acoustic modes in a cylindrical model that predicted the performance of passive control schemes through the prediction of acoustic potential energy.[14]

This work presents a theoretical study of the sound transmission into a finite cylinder under coupled structural and acoustic vibration. The proposed model includes internal acoustic axial modes. Particular attention of this study is focused on evaluating a dimensionless quantity, "noise reduction," for characterizing noise transmission into a small cylindrical enclosure. The paper is arranged as the follows. Section II presents the theoretical developments, which include analytical expressions of exterior and interior sound pressure for the finite cylindrical structure and the revisions to the definition of noise reduction. In Section III a numerical simulation for characterizing noise transmission into a ChamberCore cylinder are performed, which is companied with a comparison of analytical and experimental results. Some conclusions are given in the final section.

II. THEORY

The physics of the problem under study is described as follows: (1) an incident sound wave impinges upon the surface of a finite, cylindrical structure causing vibration of the shell, (2) the shell vibration induces sound pressure fluctuations including scattering and radiation pressures, (3) the radiated pressure to the interior excites vibration of the air inside the cylinder, and (4) the noise of the interior cavity in turn interacts with the structure to affect the structural vibration and creates the coupled vibration. The purpose of this section is to find an analytical solution to describe the exterior and interior sound pressure of the cylinder under sound wave incident.

The calculation of exterior pressure over the outside shell is a near-field problem, which is difficult to analytically solve for a finite, elastic, cylindrical shell.[15] In this study, the near-field pressure of an infinite elastic cylindrical shell is used to approximate that of the finite one. The internal sound pressure field is solved by means of the coupled structural and acoustic vibration under the input of the solved external pressure using the modal-interaction method.[13,16-18] In order to simplify analysis, the impinging wave is selected to be an oblique plane wave, and time-dependant variables are assumed to be harmonic. The solutions of external and internal pressures are presented in following several sections.

A. Exterior Pressure of an Infinite Elastic Cylindrical Shell

The specific problem studied is shown in Fig. 1. Consider an oblique plane wave impinging upon an infinite thin cylindrical shell approaching from the radial plane ($\phi = \pi$). The density of the fluid and the speeds of sound are ρ_1, c_1 and ρ_2, c_2, in the external and internal media, respectively. In the analysis of exterior pressure field, all waves will be assumed to have the same dependence on the axial coordinate z.

The incident plane sound wave can be represented as

$$p_i(x,z,t) = P_i e^{j(\omega t - k_{1x}x - k_{1z}z)}, \tag{1}$$

where P_i is the amplitude of incident sound pressure, k_{1x} and k_{1z} are the x-component and z-component of the wavenumber, respectively, and are computed from

$$\begin{cases} k_{1x} = k_1 \cos\theta \\ k_{1z} = k_1 \sin\theta \end{cases}, \tag{2}$$

where $k_1 = \omega/c_1$ is the wavenumber in the external fluid medium, and θ is the incident angle. The expansion of Eq. (1) into a cylindrical coordinate system gives[11,15,19]

$$p_i(x,z,t) = P_i e^{j(\omega t - k_{1z} z)} \sum_{m=0}^{\infty} \varepsilon_m (-j)^m J_m(k_{1r} r) \cos m\phi , \tag{3}$$

where J_m is the Bessel function of the first kind of integer order m, $k_{1\mathrm{r}} = k_{1x}$ the radial component of the wavenumber, and ε_m the Neumann factor given by

$$\varepsilon_m = \begin{cases} 1 & (m = 0) \\ 2 & (m \geq 1) \end{cases}. \tag{4}$$

The total exterior sound pressure field of the infinite cylindrical structure can be written as

$$p_{ext} = p_i + p_{se} , \tag{5}$$

where p_{ext} is the exterior pressure, p_i the incident pressure, p_{se} the scattered pressure by the elastic shell, which contains two parts:

$$p_{se} = p_{s\infty} + p_{re} , \tag{6}$$

where $p_{s\infty}$ is the scattered pressure by a rigid-cylinder with infinite acoustic impedance, and p_{re} is the pressure radiated by an elastic cylindrical shell. The general result of sound radiation from a vibrating structure is presented in the next section.

B. Radiation of a Vibrating Cylindrical Shell

Assuming that an elastic cylindrical shell is vibrating with a surface-harmonic acceleration distribution $\ddot{w}(r = a, \phi, z, t)$, which can be expanded into a Fourier series as[11,15,19]

$$\ddot{w}(r=a,\phi,z,t)=e^{-jk_{1z}z}\sum_{m=0}^{\infty}\ddot{W}_m(t)\cos(m\phi)\,, \tag{7}$$

where a is the radius of the midsurface, k_{1z} the z-components of the wavenumber given by Eq. (2), and $\ddot{W}_m(t)$ the time dependent part of the acceleration. Only the configuration in even ϕ is considered in Eq. (7). If the ϕ axis cannot be oriented to be consistent with this configuration, then a sine series is required using the same procedure presented here.

In a linear sound field without loss the pressure (p) and the particle velocity ($\overline{u}$) satisfy wave equation[15]

$$\overline{\nabla}p=-\rho\frac{\partial\overline{u}}{\partial t}\,. \tag{8}$$

The boundary condition where the fluid meets the structure is governed in the normal direction by

$$\left.\frac{\partial p(r,\phi,z,t)}{\partial r}\right|_{r=a}=-\rho\ddot{w}(r=a,\phi,z,t)\,, \tag{9}$$

where $\ddot{w}(r=a,\phi,z,t)$ is the fluid particle acceleration of the boundary. Note that the fluid particle vibration uses the same symbol as the shell vibration because it equates the shell vibration at structure-fluid boundaries. In order to satisfy the boundary condition, the radiation pressure field is therefore expressed as the series[11,15]

$$p_r(r,\phi,z,t)=e^{-jk_{1z}z}\sum_{m=0}^{\infty}P_m\left(t\right)H_m^{(2)}\left(k_{1r}r\right)\cos(m\phi)\,, \tag{10}$$

where $H_m^{(2)}$ is a Hankel function of the second kind of m order. Substituting Eqs. (10) and (7) into (9), the coefficients $P_m(t)$ are solved from

$$P_m\left(t\right)=-\frac{\rho_1\ddot{W}_m(t)}{k_{1r}H_m^{(2)\prime}\left(k_{1r}a\right)}\,, \tag{11}$$

where $(\ )'$ denotes the spatial derivative. The radiation pressure field is thus found to be

$$p_r(r,\phi,z,t) = -e^{-jk_{1z}z}\frac{\rho_1}{k_{1r}}\sum_{m=0}^{\infty}\frac{\ddot{W}_m(t)}{H_m^{(2)\prime}(k_{1r}a)}H_m^{(2)}(k_{1r}r)\cos(m\phi). \tag{12}$$

Because $W_m(t)$ is time harmonic, the surface pressure obtained from Eq. (12) can be written in terms of modal specific acoustic impedance, z_m, as[15]

$$p_r(r=a,\phi,z,t) = e^{-jk_{1z}z}\sum_{m=0}^{\infty}\dot{W}_m(t)z_m\cos(m\phi), \tag{13}$$

where

$$\dot{W}_m(t) = -\frac{j\ddot{W}_m(t)}{\omega}, \tag{14}$$

$$z_m = -\frac{j\omega\rho_1 H_m^{(2)}(k_{1r}a)}{k_{1r}H_m^{(2)\prime}(k_{1r}a)}. \tag{15}$$

The scattered pressure from an infinite rigid and elastic cylindrical shell is solved in the next two sections using the results of Section B.

C. Scattering from an Infinite Rigid Cylindrical Shell

When the boundary is rigid and there is no loss of air, the resultant particle acceleration at the boundary must have a zero component along the normal direction to the boundary:

$$\ddot{w}_{s\infty}(r=a,\phi,z,t) + \ddot{w}_i(r=a,\phi,z,t) = 0, \tag{16}$$

where $\ddot{w}_{s\infty}(r=a,\phi,z,t)$ is the scatting fluid particle acceleration at boundary ($r = a$), which is equal to the normal rigid surface acceleration, and $\ddot{w}_i(r=a,\phi,z,t)$ the normal incident fluid particle acceleration at the boundary. This acceleration is given by wave equation (8) or boundary condition Eq. (9)

$$\ddot{w}_i(r=a,\phi,z,t) = -\frac{1}{\rho_1}\frac{\partial p_i(r,\phi,z,t)}{\partial r}\bigg|_{r=a}. \tag{17}$$

Combining Eqs. (3), (16) and (17), the rigid surface acceleration is obtained as

$$\ddot{w}_{s\infty}(r=a,\phi,z,t) = P_i(t)e^{-jk_{1z}z}\frac{k_{1r}}{\rho_1}\sum_{m=0}^{\infty}\varepsilon_m(-j)^m J_m'\left(k_{1r}a\right)\cos m\phi, \tag{18}$$

where ε_m is the Neumann factor given by Eq. (4). Comparing Eq. (18) with Eq. (7), the coefficient $\ddot{W}_{s\infty,m}(t)$ is solved for:

$$\ddot{W}_{s\infty,m}(t) = P_i(t)\frac{k_{1r}}{\rho_1}\varepsilon_m(-j)^m J_m'\left(k_{1r}a\right). \tag{19}$$

Substituting Eq. (19) into Eq. (12), the scattered pressure from an infinite rigid cylindrical shell is obtained as

$$p_{s\infty}(r,\phi,z,t) = P_i(t)e^{-jk_{1z}z}\sum_{m=0}^{\infty}\varepsilon_m(-j)^m A_m H_m^{(2)}\left(k_{1r}r\right)\cos(m\phi), \tag{20}$$

where

$$A_m = -\frac{J_m'\left(k_{1r}a\right)}{H_m^{(2)\prime}\left(k_{1r}a\right)}. \tag{21}$$

The resultant pressure on the cylindrical surface required by analyzing the scattering action of elastic cylindrical shells, is the sum of the incident and scattered waves of the rigid cylinder ($p = p_i + p_{s\infty}$). Considering the following relation[1]

$$J_m(x)H_m^{(2)\prime}(x) - J_m'(x)H_m^{(2)}(x) = -j\frac{2}{\pi x}, \tag{22}$$

the pressure is calculated from

$$p(r=a,\phi,z,t)=\frac{2P_i(t)}{\pi a k_{1r}}e^{-jk_{1z}z}\sum_{m=0}^{\infty}\varepsilon_m(-j)^{m+1}\frac{1}{H_m^{(2)\prime}\left(k_{1r}a\right)}\cos(m\phi)\,. \tag{23}$$

D. Scattering from an Infinite Elastic Cylindrical Shell

The normal response of the elastic cylindrical shell under the influence of ($p = p_i + p_{s\infty}$) can be expressed in terms of modal mechanical and acoustic impedance as[15]

$$\dot{w}(r=a,\phi,z,t)=e^{-jk_{1z}z}\sum_{m=0}^{\infty}\frac{P_m(t)}{z_m+Z_m}\cos(m\phi)\,, \tag{24}$$

where $P_m(t)$ can be obtained from Eq. (23) as

$$P_m(t)=\frac{2P_i(t)}{\pi a k_{1r} H_m^{(2)\prime}\left(k_{1r}a\right)}\varepsilon_m(-j)^{m+1}, \tag{25}$$

and z_m is the modal specific acoustic impedance, and can be obtained from Eq. (15), Z_m is the modal mechanical impedance, and can be determined from the Donnell-Mushtari equations with Flügge modifying constants[20] under the absence of the fluid loading inside cylinder, which leads to the expression in the form[15]

$$Z_m = j\frac{c_p\rho_s h}{a}\frac{\left[\Omega^2-(\Omega_m^{(1)})^2\right]\left[\Omega^2-(\Omega_m^{(2)})^2\right]}{\Omega(\Omega^2-m^2)}, \tag{26}$$

where ρ_s is the volume density of the shell material, $c_p=\sqrt{E/\rho_p(1-\mu^2)}$ is the speed of sound propagating in the shell, a is the radius of midsurface, h is the thickness of the shell, $\Omega=\omega a/c_p$ is a dimensionless frequency parameter, $\Omega_m^{(1)}$, and $\Omega_m^{(2)}$ are the resonance frequencies of a thin cylindrical shell without axial component of displacement, and they are defined as[15]

$$\Omega_m^{(1)} = \frac{1}{2}\left[1 + m^2 + \beta m^4 - \sqrt{\left(1 + m^2 + \beta m^4\right)^2 - 4\beta m^6}\right], \tag{27}$$

$$\Omega_m^{(2)} = \frac{1}{2}\left[1 + m^2 + \beta m^4 + \sqrt{\left(1 + m^2 + \beta m^4\right)^2 - 4\beta m^6}\right], \tag{28}$$

where $\beta = h^2/12a^2$ is a dimensionless constant.

The coefficients of the surface-harmonic acceleration distribution can be obtained from Eq. (24):

$$\ddot{W}_m(t) = \frac{j\omega P_m(t)}{z_m + Z_m}. \tag{29}$$

Substituting Eq. (29) into Eq. (12), the radiation pressure from the infinite elastic cylindrical shell is

$$p_{re}(r,\phi,z,t) = P_i(t) e^{-jk_{1z}z} \sum_{m=0}^{\infty} \varepsilon_m (-j)^m B_m H_m^{(2)}\left(k_{1r}a\right) \cos(m\phi), \tag{30}$$

where

$$B_m = -\frac{2\rho_1\omega}{\pi a k_{1r}^2 (z_m + Z_m)\left[H_m^{(2)\prime}\left(k_{1r}a\right)\right]^2}. \tag{31}$$

Finally, the external pressure for the infinite elastic cylindrical shell is computed from

$$p_{ext}(r,\phi,z,t) = p_i(r,\phi,z,t) + p_{s\infty}(r,\phi,z,t) + p_{re}(r,\phi,z,t). \tag{32}$$

Substituting Eqs. (3), (20) and (30) into Eq. (32), yields

$$p_{ext}(r,\phi,z,t) = P_i(t) e^{-jk_{1z}z} \sum_{m=0}^{\infty} \varepsilon_m (-j)^m \left[J_m\left(k_{1r}a\right) + C_m H_m^{(2)}\left(k_{1r}a\right)\right] \cos(m\phi), \tag{33}$$

where $C_m = A_m + B_m$, and A_m and B_m are given by Eqs. (21) and (31), respectively.

When the incident pressure is time harmonic, i.e. $P_i(t) = P_i e^{j\omega t}$, the external pressure over the infinite flexible cylindrical shell is

$$p_{ext}(r=a,\phi,z,t) = P_i e^{j\omega t - jk_{1z}z} \sum_{m=0}^{\infty} \varepsilon_m (-j)^m \left[J_m\left(k_{1r}a\right) + C_m H_m^{(2)}\left(k_{1r}a\right) \right] \cos(m\phi), \tag{34}$$

where P_i is the magnitude of incident pressure. This concludes the derivation for the external pressure field.

E. Interior Pressure of a Finite Elastic Cylindrical Shell

It is assumed that the end caps of the finite cylindrical structure are rigid, so that only the radial motion of the curved surface of the cylindrical structure excites the acoustic cavity (see Fig. 2). The modal-interaction approach[13,16-18] is used to calculate the sound pressure inside the cavity under the excitation of external pressure which is approximated by the one obtained from the infinite cylindrical shell [see Eq. (34)]. Only the normal motion of the cylindrical shell is considered to excite the cavity acoustics, and only the even ϕ configuration is considered. Note that either odd [sin($m\phi$) modes] or even [cos($m\phi$) modes] can be chosen, since the $\phi=0^\circ$ direction is arbitrary.

For a simply supported cylindrical structure without axial constraint, the harmonic radial displacement of the shell, subject to external pressure excitation, is described as a linear combination of the *in vacuo* normal modes as

$$w(r=a,\phi,z,t)=\sum_{o=0}^{\infty}\sum_{q=1}^{\infty}W_{oq}(t)\Phi_{oq}(\phi,z)\,, \tag{35}$$

where o is the number of circumferential waves in the structural mode shapes, and q is the number of longitudinal half-waves in the structural mode shapes. The *in-vacuo* structural normal mode shapes can be written as[21]

$$\Phi_{oq}(\phi,z)=\cos(o\phi)\sin\left(q\frac{\pi}{L}z\right), \tag{36}$$

where L is the length of the finite cylindrical shell. The natural frequencies for simply-supported closed thin shells can be obtained from Leissa's book.[21]

The modal equation for the structure can then be derived by taking advantage of the orthogonal properties of the mode shapes as[16]

$$\ddot{W}_{oq}(t)+2\xi_{oq}^{s}\omega_{oq}^{s}\dot{W}_{oq}(t)+(\omega_{oq}^{s})^{2}W_{oq}(t)=\frac{S}{\mathrm{M}_{oq}}\sum_{l,m,n=0}^{\infty}P_{lmn}(t)D_{oq,lmn}+\frac{p_{oq}(t)}{\mathrm{M}_{oq}}. \tag{37}$$

In the right hand side of Eq. (37), the first term is the cavity fluid loading, and the second term is the external distributed input, where M_{oq} is modal mass of the structure, $D_{oq,lmn}$ is the dimensionless structural-acoustic coupling coefficient, $p_{oq}(t)$ is the modal force from the external pressure field, $P_{lmn}(t)$ is the time-dependent portion of the interior pressure, l, m and n are the number of radial nodes, diametric nodes and longitudinal nodes in acoustic cavity mode shapes, respectively, and $S=2\pi aL$ is the area of the midsurface of the cylindrical shell. M_{oq}, $D_{oq,lmn}$, and $p_{oq}(t)$ are given by the following equations, respectively:

$$\mathrm{M}_{oq}=\int_{S}m_{s}\Phi_{oq}^{2}(\phi,z)dS\,, \tag{38}$$

$$D_{oq,lmn} = \frac{1}{S} \int_S \Phi_{oq}(\phi, z) \Psi_{lmn}(r = a, \phi, z)\, dS \,, \tag{39}$$

$$p_{oq}(t) = \int_S p_{ext}(r = a, \phi, z, t) \Phi_{oq}(\phi, z)\, dS = P_i e^{j\omega t} E_{oq} \,, \tag{40}$$

where the structural mode shapes Φ_{oq} are given by Eq. (36), Ψ_{lmn} are the acoustic mode shapes, which are defined by Eq. (46), and the pressure p_{ext} is given by Eq. (34). For a uniform cylindrical shell with surface density m_s, coefficients M_{oq}, $D_{oq,lmn}$, and E_{op} become:

$$\mathrm{M}_{oq} = \frac{1}{\varepsilon_o} m_s L a \pi \,, \tag{41}$$

$$D_{oq,lmn} = \begin{cases} \dfrac{aL}{S\varepsilon_m} J_m\left(k_{lm} a\right) \left[\dfrac{1 - \cos(q+n)\pi}{q+n} + \dfrac{1 - \cos(q-n)\pi}{q-n} \right], & (o = m \text{ and } q \neq n) \\ 0, & \text{otherwise} \end{cases} , \tag{42}$$

$$E_{oq} = \begin{cases} (-j)^{o+1} aL\pi \left[J_o\left(k_{1r} a\right) + C_o H_o^{(2)}\left(k_{1r} a\right) \right], & \left(k_{1z} = q\dfrac{\pi}{L} \right) \\ (-j)^{o} aL\pi \left[J_o\left(k_{1r} a\right) + C_o H_o^{(2)}\left(k_{1r} a\right) \right] \left\{ \left[\dfrac{-\cos\left(k_{1z} L + q\pi\right) + 1}{k_{1z} L + q\pi} + \dfrac{\cos\left(k_{1z} L - q\pi\right) - 1}{k_{1z} L - q\pi} \right] + j \left[\dfrac{\sin\left(k_{1z} L + q\pi\right)}{k_{1z} L + q\pi} - \dfrac{\sin\left(k_{1z} L - q\pi\right)}{k_{1z} L - q\pi} \right] \right\}, & \text{otherwise} \end{cases} \tag{43}$$

where ε_o and ε_m are the Neumann factor given by Eq. (4).

If the cavity fluid loading is neglected, Eq. (37) becomes

$$\ddot{W}_{oq}(t) + 2\xi_{oq}^s \omega_{oq}^s \dot{W}_{oq}(t) + (\omega_{oq}^s) W_{oq}(t) = \frac{P_i E_{oq}}{\mathrm{M}_{oq}} e^{j\omega t} \,. \tag{44}$$

The effects on the noise transmission into the cylinder due to ignoring cavity fluid loading will be discussed in Section III through comparing analytical and experimental results. Next, the cylindrical cavity acoustic effects induced by the elastic shell vibration are studied.

The acoustic pressure in the cavity can be expressed as a linear combination of the rigid-wall acoustic cavity modes:

$$p(r,\phi,z,t)=\sum_{l,m,n=0}^{\infty}P_{lmn}(t)\Psi_{lmn}(r,\phi,z)\,. \tag{45}$$

The cylindrical acoustic cavity mode shapes are[21]

$$\Psi_{lmn}(r,\phi,z)=J_m\left(k_{lm}r\right)\cos(m\phi)\cos\left(n\frac{\pi}{L}z\right). \tag{46}$$

Note that *l*, *m*, and *n* cannot be zero at the same time, because the static pressure mode (0, 0, 0) is not considered in this study. k_{lm} is solved from $J'_{lm}(k_{lm}r)|_{r=a}=0$, and the acoustic natural frequencies are obtained from $\omega^f_{lmn}=c_2\sqrt{k^2_{lm}+(n\frac{\pi}{L})^2}$, where the superscript f denotes "fluid".

Invoking the orthogonality condition for mode shapes and considering the damping term, the modal equation for the acoustic system is written as[16]

$$\ddot{P}_{lmn}(t)+2\xi^f_{lmn}\omega^f_{lmn}\dot{P}_{lmn}(t)+(\omega^f_{lmn})^2P_{lmn}(t)=-\frac{\rho_2c_2^2S}{V_{lmn}}\sum_{o=0,q=1}^{\infty}\ddot{W}_{oq}(t)D_{oq,lmn}\ , \tag{47}$$

where V_{lmn} is the modal volume, and is calculated by

$$V_{lmn}=\int_V\Psi^2_{lmn}(r,\phi,z)dV\ , \tag{48}$$

where V is the acoustic cavity volume. For a cylindrical cavity with length L and midsurface radius a, the modal volume is computed from

$$V_{lmn}=\begin{cases}\dfrac{\pi a^2L}{2}, & l=m=0,n\in[1,\infty)\\ \dfrac{\pi a^2L}{\varepsilon_m\varepsilon_n}\left\{\left[J'_m\left(k_{lm}a\right)\right]^2+\left[1-\left(\dfrac{m}{k_{lm}a}\right)^2\right]\left[J_m\left(k_{lm}a\right)\right]^2\right\}, & \text{otherwise}\end{cases}. \tag{49}$$

Because all time-dependent variables are assumed to be time harmonic, the displacement and pressure are expressed as $W_{oq}(t) = W_{oq} e^{j\omega t}$ and $P_{lmn}(t) = P_{lmn} e^{j\omega t}$. Solving Eqs. (44) and (47) for the modal pressure distribution $P_{lmn}(t)$, yields

$$P_{lmn}(t) = P_i e^{j\omega t} \frac{F_{lmn}(\omega)}{\left[-\omega^2 + j2\xi_{lmn}^f \omega_{lmn}^f \omega + \left(\omega_{lmn}^f\right)^2\right] V_{lmn}}, \tag{50}$$

where

$$F_{lmn}(\omega) = \rho_2 c_2^2 S \sum_{o=0,q=1}^{\infty} \left[\frac{E_{oq} D_{oq,lmn}}{\left\{ \left[\left(\frac{\omega_{oq}^s}{\omega} \right)^2 - 1 \right] + j2\xi_{oq}^s \frac{\omega_{oq}^s}{\omega} \right\} \mathrm{M}_{oq}} \right]. \tag{51}$$

Substituting Eq. (50) into Eq. (45), the internal pressure field is

$$p_{int}(r,\phi,z,t) = P_i e^{j\omega t} \sum_{l,m,n=0}^{\infty} \frac{F_{lmn}(\omega)}{\left[-\omega^2 + j2\xi_{lmn}^f \omega_{lmn}^f \omega + (\omega_{lmn}^f)^2\right] V_{lmn}} \Psi_{lmn}(r,\phi,z). \tag{52}$$

The structural damping ξ^s and fluid medium damping ξ^f in Eq. (52) are determined by experimental modal identification. [1]

In order to derive an analytical solution for the noise reduction of the finite cylindrical structure, the modal pressure (P_{lmn}) is re-expressed as:[1]

$$P_{lmn}(t) = P_i e^{j\omega t} \left(G_{lmn}^R + jG_{lmn}^I \right), \tag{53}$$

where G^R_{lmn} and G^I_{lmn} are the real part and imaginary part of ($F_{lmn}(\omega)/[-\omega^2 + j2\xi^f_{lmn}\omega^f_{lmn}\omega + (\omega^f_{lmn})^2]V_{lmn}$), respectively.[1] Then, the internal pressure field is re-written as:

$$p_{int}(r,\phi,z,t) = P_i e^{j\omega t} \sum_{l,m,n=0}^{\infty} \left(G^R_{lmn} + jG^I_{lmn} \right) \Psi_{lmn}(r,\phi,z) . \tag{54}$$

Equations (34) and (54) are used in the calculation of noise reduction in the next section.

F. Noise Reduction

The definition of transmission loss (*TL*) for an infinite flat panel assumes that the transmitted sound is totally absorbed, and only inward-propagating waves exist. However, the problem under consideration differs from the infinite flat panel, not only because of its finite dimension, but also because of the effects of internal acoustic cavity resonances in the closed cylindrical shell. Hence, it is not possible to define a transmission loss as is done for flat panels. For measurement of the sound transmission through cylindrical shells, Holmer and Heymann[22] defined the sound power transmission coefficient to be equal to the ratio of power radiated per unit surface area of the shell to the power passing axially through a unit area of cross section. In other references,[11, 13, 23-25] researchers suggested using the noise reduction instead of calculating *TL*, which was equaled the ratio of the outer time- and surface-averaged mean-square pressure and inner time- and volume-averaged mean-square pressure. In this study, the revised noise reduction for characterizing broadband sound transmission into a finite cylindrical structure is defined as the ratio of external time- and surface-averaged mean-square pressure over the internal time- and surface-averaged mean-square pressure, which is computed from

$$NR = -\log_{10} \frac{\left\langle p_{int}^2 (r,\phi,z,t) \right\rangle}{\left\langle p_{ext}^2 (r,\phi,z,t) \right\rangle}, \tag{55}$$

where $\left\langle p^2 (r,\phi,z,t) \right\rangle$ is the mean-square pressure of $p(r, \phi, z, t)$ averaged over the midsuface area for a thin wall structure, S, and a time period, T. It is defined as

$$\left\langle p^2 (r,\phi,z,t) \right\rangle = \frac{1}{S\,T} \int_S \int_T p(r,\phi,z,t) p^*(r,\phi,z,t) dtdS, \tag{56}$$

where $(\ )^*$ denotes the complex conjugate. For a cylindrical shell, the expression of dS in Eq. (56) is: $dS = rd\phi dz$, and the mean-square external pressure averaged over the midsurface area, S and time period, T is calculated from

$$\left\langle p_{ext}^2 (r,\phi,z,t) \right\rangle = P_i^2 \Pi(\omega), \tag{57}$$

$$\Pi(\omega) = \sum_{m=0}^{\infty} \varepsilon_m \left| J_m(k_{1r}a) + C_m H_m^{(2)}(k_{1r}a) \right|^2 . \tag{58}$$

The mean-square internal pressure averaged over the midsurface area, S and time period, T is calculated from

$$\left\langle p_{int}^2 (r,\phi,z,t) \right\rangle = \frac{1}{S} P_i^2 \int_S \left\{ \underbrace{\sum_{l,m,n=0}^{\infty} \left[\left(G_{lmn}^R \right)^2 + \left(G_{lmn}^I \right)^2 \right] \Psi_{lmn}^2}_{\text{term 1}} + \underbrace{\sum_{o=0,o\neq l}^{\infty} \sum_{l,m,n=0}^{\infty} \left(G_{lmn}^R G_{omn}^R + G_{lmn}^I G_{omn}^I \right) \Psi_{lmn} \Psi_{omn}}_{\text{term 2}} \right\} rd\phi dz . \tag{59}$$

The integration of the "term 1" in Eq. (59) over the midsurface yields:

$$\begin{aligned} &\int_S \sum_{l,m,n=0}^{\infty} \left[\left(G_{lmn}^R \right)^2 + \left(G_{lmn}^I \right)^2 \right] \Psi_{lmn}^2 rd\phi dz = aL\pi \sum_{n=1}^{\infty} \left[\left(G_{00n}^R \right)^2 + \left(G_{00n}^I \right)^2 \right] \\ &+ aL\pi \sum_{l=0,m=1,n=0}^{\infty} \frac{1}{\varepsilon_n} \left[\left(G_{lmn}^R \right)^2 + \left(G_{lmn}^I \right)^2 \right] J_m^2(k_{lm}a) + 2aL\pi \sum_{l=1,m=0,n=0}^{\infty} \frac{1}{\varepsilon_m \varepsilon_n} \left[\left(G_{lmn}^R \right)^2 + \left(G_{lmn}^I \right)^2 \right] J_m^2(k_{lm}a) \end{aligned} . \tag{60}$$

The integration of the "term 2 in Eq. (59) over the midsurface yields:

$$\int_S \sum_{\substack{l,m,n,o=0\\ o\neq l}}^{\infty}\left(G^R_{lmn}G^R_{omn}+G^I_{lmn}G^I_{omn}\right)\Psi_{lmn}\Psi_{omn}r d\phi dz = aL\pi\sum_{n,o=1}^{\infty}\left(G^R_{00n}G^R_{o0n}+G^I_{00n}G^I_{o0n}\right)J_m(k_{om}a)$$
$$+aL\pi\sum_{o=0,o\neq l}^{\infty}\;\sum_{l=0,m=1,n=0}^{\infty}\frac{1}{\varepsilon_n}\left(G^R_{lmn}G^R_{omn}+G^I_{lmn}G^I_{omn}\right)J_m(k_{lm}a)J_m(k_{om}a) \tag{61}$$
$$+2aL\pi\sum_{o=0,o\neq l}^{\infty}\;\sum_{l=1,m=0,n=0}^{\infty}\frac{1}{\varepsilon_m\varepsilon_n}\left(G^R_{lmn}G^R_{omn}+G^I_{lmn}G^I_{omn}\right)J_m(k_{lm}a)J_m(k_{om}a)$$

Substituting Eqs. (60) and (61) and $S = 2\pi aL$ into (59), yields

$$\left\langle p^2_{int}(r,\phi,z,t)\right\rangle = P_i^2\Theta(\omega)\,, \tag{62}$$

where

$$\Theta(\omega)=\frac{1}{2}\sum_{n=1}^{\infty}\left[\left(G^R_{00n}\right)^2+\left(G^I_{00n}\right)^2\right]+\frac{1}{2}\sum_{l=0,m=1,n=0}^{\infty}\frac{1}{\varepsilon_n}\left[\left(G^R_{lmn}\right)^2+\left(G^I_{lmn}\right)^2\right]J^2_m(k_{lm}a)$$
$$+\sum_{l=1,m=0,n=0}^{\infty}\frac{1}{\varepsilon_m\varepsilon_n}\left[\left(G^R_{lmn}\right)^2+\left(G^I_{lmn}\right)^2\right]J^2_m(k_{lm}a)+\frac{1}{2}\sum_{n,o=1}^{\infty}\left(G^R_{00n}G^R_{o0n}+G^I_{00n}G^I_{o0n}\right)J_m(k_{om}a)$$
$$+\frac{1}{2}\sum_{o=0,o\neq l}^{\infty}\;\sum_{l=0,m=1,n=0}^{\infty}\frac{1}{\varepsilon_n}\left(G^R_{lmn}G^R_{omn}+G^I_{lmn}G^I_{omn}\right)J_m(k_{lm}a)J_m(k_{om}a) \tag{63}$$
$$+\sum_{o=0,o\neq l}^{\infty}\;\sum_{l=1,m=0,n=0}^{\infty}\frac{1}{\varepsilon_m\varepsilon_n}\left(G^R_{lmn}G^R_{omn}+G^I_{lmn}G^I_{omn}\right)J_m(k_{lm}a)J_m(k_{om}a)$$

Substituting Eqs (57) and (62) into Eq. (55), the analytical formula for the calculation of noise reduction is obtained as

$$NR = 10\log_{10}\frac{\Pi(\omega)}{\Theta(\omega)}. \tag{64}$$

The *NR* into a cylindrical structure under a plane wave impinging with an incident angle, θ, is only a function of frequency since the time variable disappeared from the integrations (as does spatial dependence), and the amplitude of incident plane wave was also canceled during the calculation of the internal and external mean-square pressure ratio. Note that the noise reduction given by Eq. (64) is only used to characterize the noise transmission into a finite, thin, cylindrical enclosure with two rigid-ends, and also note that the equations are derived with the internal fluid loading ignored (assumed to be light) and with an oblique plane incident wave.

The definition of *NR* proposed in this paper is more similar to *TL* than previous definitions and it is more amenable to comparing with experimental measurements. While only the radiation is considered in the transmitted wave for the *TL*, in the *NR*, the transmitted sound includes both radiation and the scattered waves inside the acoustic cavity. Note that transmission loss and noise reduction are dimensionless quantities that are typically expressed in decibels.

III. NUMERICAL SIMULATION

Numerical results from Eq. (64) have been generated for the ChamberCore composite cylindrical shell with radius $a = 255$ mm, effective thickness $h = 20.1$ mm, and length $L = 760$ mm. The physical parameters of the composite material have been homogenized and are: Young's modulus $E = 60$ GPa, Poisson's ratio $\mu = 0.3$, effective density of the uniform shell is $\rho_s = 315$ kg/m^3. The speed of sound and the density of air inside and outside the cylindrical shell are $c_1 = c_2 = 346$ m/s (at 75° F) and $\rho_1 = \rho_2 = 1.21$ kg/m^3. The oblique incident plane wave is given by Eq. (1), where $\theta = 30°$. In order to simplify analysis, the acoustic damping ratio was set to the same value for all modes and obtained by averaging the measured results (0.28%).[1,12] The structural damping ratio was also set to the same for all modes and obtained by averaging the identification results (4.64%).[1,12] The maximum order of acoustic and structural modes is set to six per each index in the simulation for a total of 36 structural modes and 216 acoustic cavity modes. The analytical results for the first ten acoustic modes and natural frequencies of the cavity formed by the closed cylindrical structure are listed in Table I.

Fig. 3 shows the curves of the noise reduction given by Eq. (64) at θ = 30°, with frequency range [0, 3,000] Hz and a logarithmic abscissa. The first ten acoustic cavity resonances are also indicated in the figure as dashed vertical lines. From Figure 3 it is observed that there are sharp dips at all cavity resonances, which is consistent with previous experimental studies.[1,3,4,12] This phenomena can be explained by examining Eqs. (52) and (55). From Eq. (52), there is a peak in the interior pressure-frequency curve at each acoustic cavity resonance frequency (ω_{lmn}^{f}), and these peaks become dips in the *NR* curve by the definition of *NR* in Eq. (55). It is concluded that the cavity resonances significantly reduce the noise reduction capability of the finite cylindrical structure, dominating the *NR* at low frequencies and even causing amplification (negative *NR*, also see Fig. 3) at 398 Hz, 455 Hz, and 458 Hz. From the figure it is also important to note that the pure longitudinal modes that were neglected in previous models, i.e. (001) at 228 Hz, (002) at 455 Hz, and (003) at 683 Hz, play a very important role in noise transmission of low frequencies. The structural resonances do not play a significant role in the *NR* results of Fig. 3 since they are higher than 4,000 Hz. Table II lists the predicted structural resonance frequencies.[21]

Figure 4 shows the effects of varying the internal acoustic damping on the *NR* for θ = 30°. The solid curve is the *NR* curve with general acoustic damping (0.0028), and the dashed curve is the *NR* curve with a ten-times increase in the general acoustic damping (0.028). From Fig. 4 it is observed that when increasing internal acoustic damping ratios the noise reduction obtains significant broadband improvement. Absorptive treatments would work well at providing increased damping at the higher frequencies, but would not at low frequencies.

Fig. 5 shows the effects of the sound incidence angle, θ, on the *NR*. The effects are more pronounced as the incidence angle approaches zero, i.e. normal to the cylindrical shell. In the following, the mechanism of how the incident angle affects the noise reduction is discussed in detail based on the normal incident sound ($\theta = 0°$) case. From Eq. (2) it can be observed that the x-component of the wavenumber is $k_{1x} = \omega / c$, and the z-component is $k_{1z} = 0$ when $\theta = 0°$. Eq. (43) is then simplifies to

$$E_{oq} = \begin{cases} (-j)^{o+1} aL\pi \left[J_o(ka) + C_o H_o^{(2)}(ka) \right], & (q = 0) \\ (-j)^{o} 4aL \left[J_o(ka) + C_o H_o^{(2)}(ka) \right] \dfrac{1}{q}, & (q = \text{odd number}) \\ 0, & (q = \text{even number}) \end{cases} . \tag{65}$$

From Eqs. (42) and (65) it is observed that when the acoustic cavity modes are purely axial (i.e. $l = 0$, $m = 0$, and $n \neq 0$), the coupled structural and acoustic vibration loading in Eq. (51) also becomes zero at these modes (i.e. $E_{oq}D_{oq,lmn} = 0$), which will in turn cause the modal pressure, Eq. (51), to be zero [i.e. $F_{lmn}(\omega) = 0$] at these modes. As a result, the purely axial cavity modes have no contribution to the internal pressure in Eq. (52) when the sound wave impinges normally upon the cylindrical shell. As the incidence angle increases, the extent of the contribution of the purely axial acoustic modes to the internal modal pressure increases, which in turn impacts the value of the *NR*. From inspecting Fig. 5, it is observed that the small incident angle creates a significant influence on the *NR* in the vicinity of the resonance frequencies of the purely axial acoustic cavity modes (001 mode at 228 Hz, 002 mode at 455 Hz, and 003 mode at 683 Hz).

Figure 6 is a comparison of analytical (Fig. 6a) and measured (Fig. 6b) results for the noise transmission into the ChamberCore cylindrical structure. As indication in the legends of the figures, the analytical *NR* is calculated with a plane wave impinging at an incident angle, $\theta =$ 30°, while the measured *NR* results are obtained in a approximately diffuse field.[1,3,4] The first ten acoustic cavity resonances are also shown in Fig. 6 as dashed vertical lines.

The measured noise reduction is calculated by an *in-situ* method developed in previous studies.[1,3,4,12] Firstly, the ChamberCore cylinder was installed in a diffuse sound field, and the autospectrum signals were measured over the outside and inside surface of the cylinder. Secondly, the noise reduction is computed by

$$NR = -10\log_{10}\frac{\left\langle p_{int}^2(\omega)\right\rangle}{\left\langle p_{ext}^2(\omega)\right\rangle}, \qquad (66)$$

where $< p_{ext}^2(\omega) >$ is the mean-square external pressure spectrum averaged over the outside shell surface, and $< p_{int}^2(\omega) >$ is the mean-square internal pressure spectrum averaged over the inside shell surface. Note that because the shell is thin, both the internal and external areas are well approximated by the mid-surface area, *S*.

From Fig. 6 it is observed that the general trends of the measured and analytical *NR* curves are very similar, while the absolute values of *NR* at low frequencies (smaller than 200 Hz) and high frequencies (larger than 1,500 Hz) has some discrepancy. There are two main reasons for the difference between the experimental and analytical results. First, the analytical *NR* was calculated for a plane wave with an incident angle of (θ = 30°), while the experimental results were measured in an approximately diffuse sound field. Second, the effects of the internal fluid loading on the *NR* are present in the experimental results, while the effects are neglected in the analytical model in order to simplify the derivation. The influence of the fluid loading on the *NR* is complex, and includes the change of both internal and external sound fields by the coupled acoustic and structural vibration. The effects of internal fluid loading and different sound fields on the *NR* would make a nice topic for a future research endeavor.

IV. CONCLUSIONS

An extended model for the noise reduction for a finite uniform cylindrical shell was developed that includes axial structural-acoustic modes. The exterior near-field pressure was approximated with that for an infinite elastic cylindrical shell. The interior pressure distribution of a finite cylindrical structure was derived using a modal model. Donnel-Mushtari and Flügge's theories were used for the structural analysis, and were coupled to the rigid-wall acoustic modes using a modal-interaction approach. Analytical results were presented for a novel ChamberCore composite fairing and compared with experimentally obtained *NR*. Both the experimental and numerical results show that the cavity resonances have a significant effect on the noise transmission into the finite cylindrical structure. A parametric study found that higher internal acoustic damping provides improved broadband noise transmission reduction. In particular, the axial modes, which were not considered in previous studies, were found to provide significant decrease in the *NR* as increase of the sound incident angle. The mechanism of effects on the *NR* of the incident angle was also presented in detail.

REFERENCE

1. D. Li, "Vibroacoustic Behavior and Noise Control Studies of Advanced Composite Structures," Ph.D. Dissertation, School of Engineering, University of Pittsburgh, Pittsburgh, PA (2003).

2. E. Herup, S. Huybrechts, S. Griffin, and S. Tsai, "Method of making composite ChamberCore sandwich-type structure with inherent acoustic attenuation," U.S. Patent No. 6,231,710 B1 (2001).

3. D. Li and J. S. Vipperman, "Noise transmission control studies on a chamber core composite cylinder," IMECE02-33069, New Orleans, LA, 2002.

4. J. S. Vipperman, D. Li, I. Avdeev, and S. A. Lane, "Investigation of the sound transmission into an advanced grid-stiffened structure," J. Vib. and Acoust., **125**, 257-266 (2003).

5. S. M. Huybrechts and T. E. Meink, "Advanced grid stiffened structures for the next generation of launch vehicles," Proceedings of Aerospace Conference, IEEE, **1**, 263 –270 (1997).

6. Y. Y. Tang, J. H. Robinson, and R. J. Silcox, "Sound transmission through two concentric cylindrical sandwich shells," 14th International Modal Analysis Conference, Dearbon, Michigan, Feb. 1996.

7. Y. Y. Tang, J. H. Robinson, and R. J. Silcox, “Sound transmission through a cylindrical sandwich shell with honeycomb core,” 34th AIAA Aerospace Sciences Meeting and Exhibit, Reno, Nevada, AIAA Paper No. 96-0877 (1996).

8. P. H. White, “Sound transmission through a finite, closed, cylindrical shell,” J. Acoust. Soc. Am., **40**, 1124-1130 (1966).

9. L. Cheng, “Fluid-structural coupling of a plate-ended cylindrical shell: vibration and internal sound field,” J. Sound Vib., **174**, 641-654 (1994).

10. Y. K. Tso and C. H. Hansen, “An investigation of the coupling loss factor for a cylinder/plate structure,” J. Sound Vib., **199**, 629-643 (1997).

11. L. R. Koval, “Effects of cavity resonances on sound transmission into a thin cylindrical shell,” J. Sound Vib., 59, 23-33 (1978).

12. D. Li and J. S. Vipperman, “On the noise transmission and control for a cylindrical ChamberCore composite structure,” accepted for publication by J. Sound Vib.

13. P. Gardonio, N. S. Ferguson, and F. J. Fahy, “A modal expansion analysis of noise transmission through circular cylindrical shell structures with blocking masses,” J. Sound Vib., **244**, 259-297 (2001).

14. S. J. Estève and M. E. Johnson, “Reduction of transmission into a circular cylindrical shell using distributed vibration absorbers and Helmholtz resonators,” J. Acoust. Soc. Am., **112**, 2840-2848 (2002).

15. M. C. Junger and D. Feit, *Sound, Structures, and Their Interaction* (2nd edition; MIT Press Cambridge, Massachusetts, London, 1986).

16. F. Fahy, *Sound and Structural Vibration: Radiation, Transmission and Response* (Academic Press, London, 1993).

17. Y. M. Huang and C. R. Fuller, "The effects of dynamic absorbers on the forced vibration of a cylindrical shell and its coupled interior sound field," J. Sound Vib., **20**, 401-418 (1997).

18. D. R. Thomas, P. A. Nelson, and S. J. Elliot, "Active control of the transmission of sound through a thin cylindrical shell, Part II: the minimization of acoustic potential energy," J. Sound Vib., **167**, 113-128 (1993).

19. N. M. McLachlan, *Bessel Functions for Engineers* (2nd edition; Oxford University Press, 1955).

20. R. D. Blevins, *Formulations for Natural Frequency and Mode Shape* (Van Nostrand Reinhold company, 1979).

21. A. W. Leissa, *Vibration of Shells*, NASA-SP-288, 1973, pp. 43-46.

22. C. I. Holmer and F. J. Heymann, "Transmission of sound through pipe walls in the presence of flow," J. Sound Vib., **70**, 275-301.

23. C. R. Fuller, S. J. Elliott, and P. A. Nelson, *Active Control of Vibration* (Academic Press, London, 1989).

24. C. R. Fuller and A. H. von Flotow, "Active control of sound and vibration", IEEE Control Systems Magazine, **15**, 9-19 (1995).

[25.] C. H. Hansen and S. D. Scott D. Snyder, *Active Control of Noise and Vibration* (E & FN Spon Press, 1997).

TABLE I. First ten acoustic cavity modes and their natural frequencies.

TABLE II. First six structural modes and their natural frequencies.

TABLE I. First ten acoustic cavity modes and their natural frequencies.

Mode No.	Mode shape order (l,m,n)	Analytical frequency (Hz)
1	001	228
2	010	398
3	002	455
4	011	458
5	012	604
6	020	660
7	003	683
8	021	698
9	013	790
10	022	801

TABLE II. First six structural modes and their natural frequencies.

Mode No.	Mode shape order (o,q)	Analytical Frequency (Hz)
1	21	4,141
2	31	4,410
3	11	5,546
4	41	5,577
5	32	5,827
6	42	6,336

FIG. 1. Geometry and incident wave of an infinite cylindrical structure.

FIG. 2. Geometry and incident wave of a finite cylindrical structure.

FIG. 3. Theoretical *NR* of a ChamberCore cylindrical fairing ($\theta = 30°$).

FIG. 4. Effects of the acoustic damping on *NR* ($\theta = 30°$).

FIG. 5. Effects of the incident angle on *NR*.

FIG. 6. Comparison of analytical (a) and measured (b) *NR* for a ChamberCore cylindrical fairing.

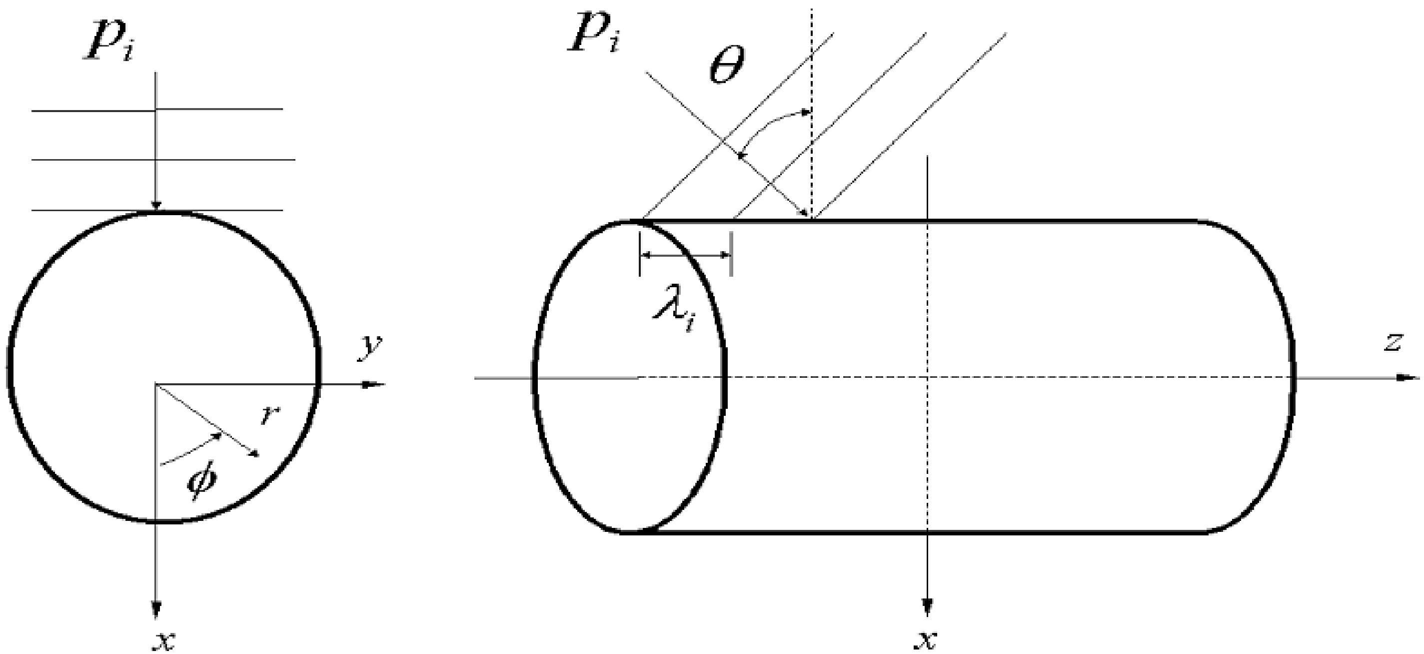

p_i
y
r
ϕ
x
p_i
θ
λ_i
z
x

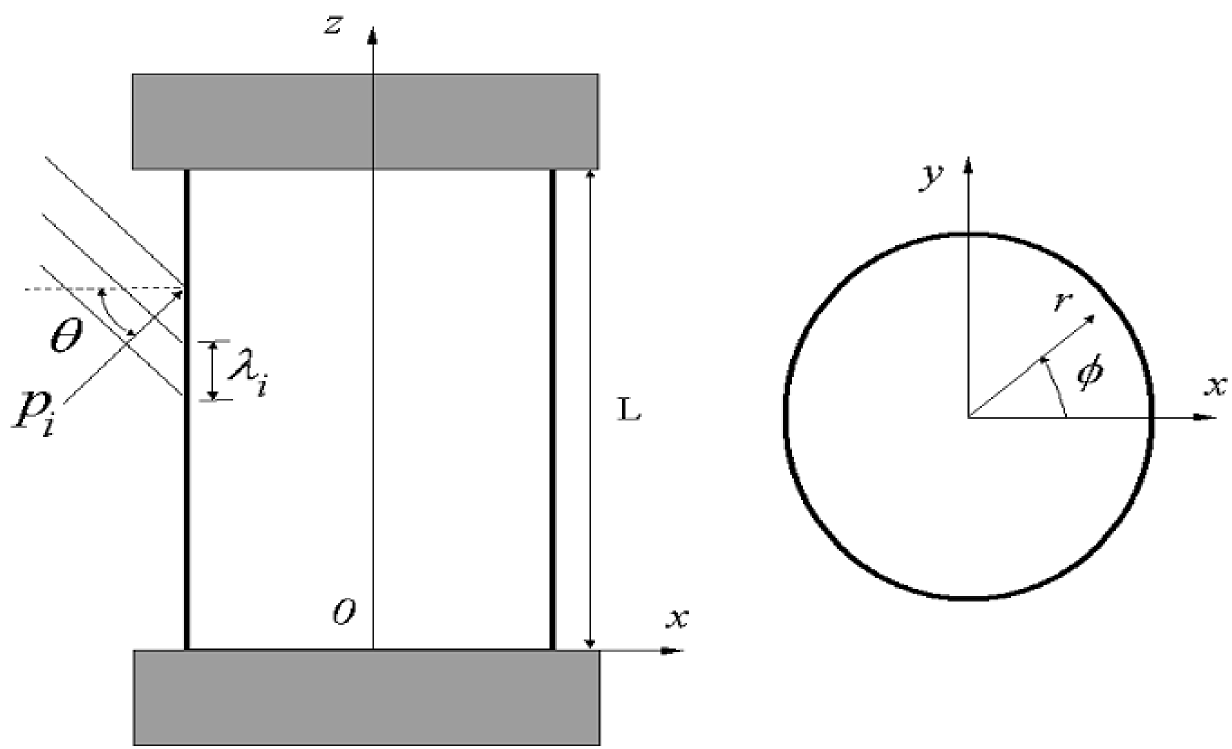
z
θ
p_i
λ_i
L
0
x
y
r
ϕ
x

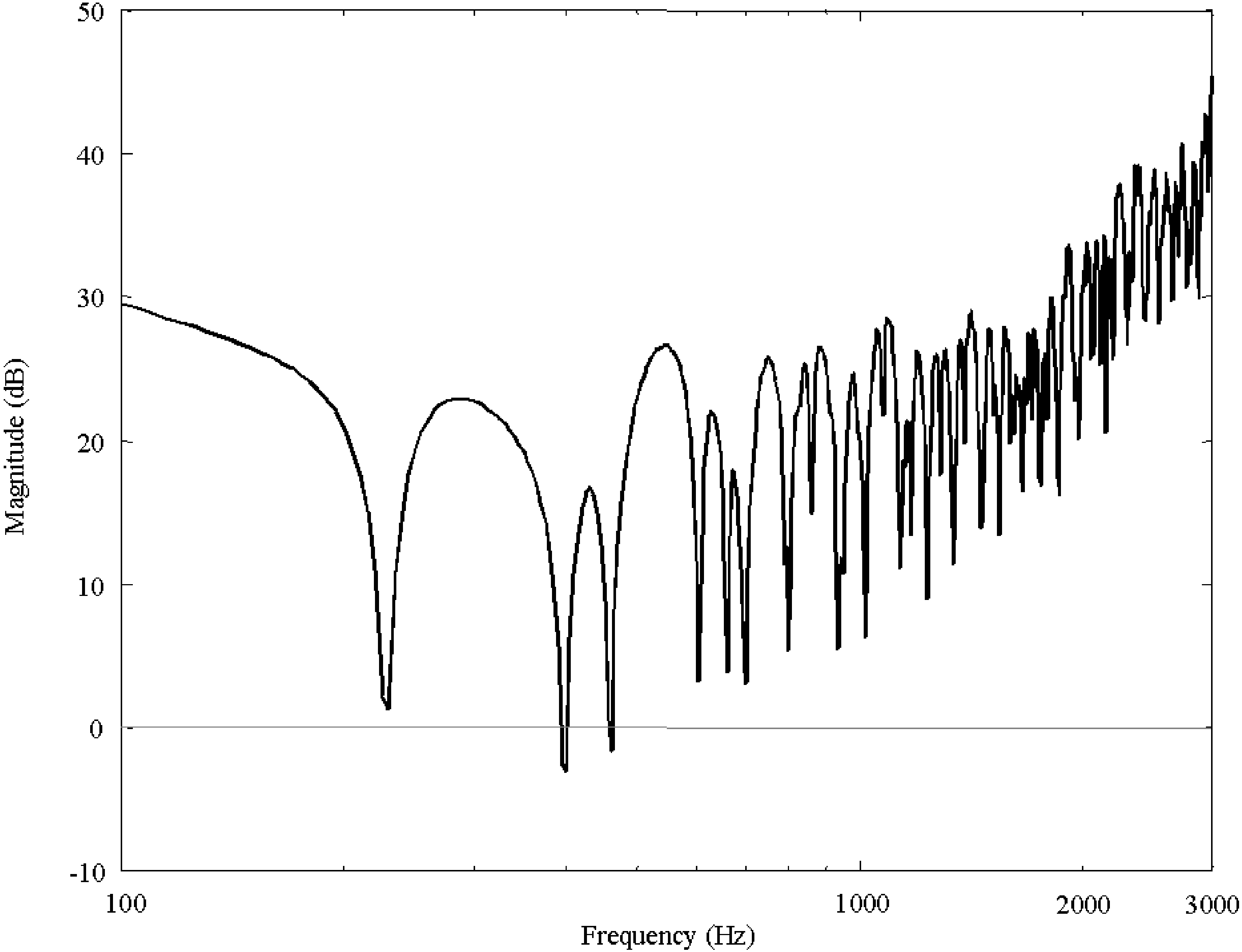

50
40
30
20
10
0
-10
Magnitude (dB)
100
1000
2000
3000
Frequency (Hz)

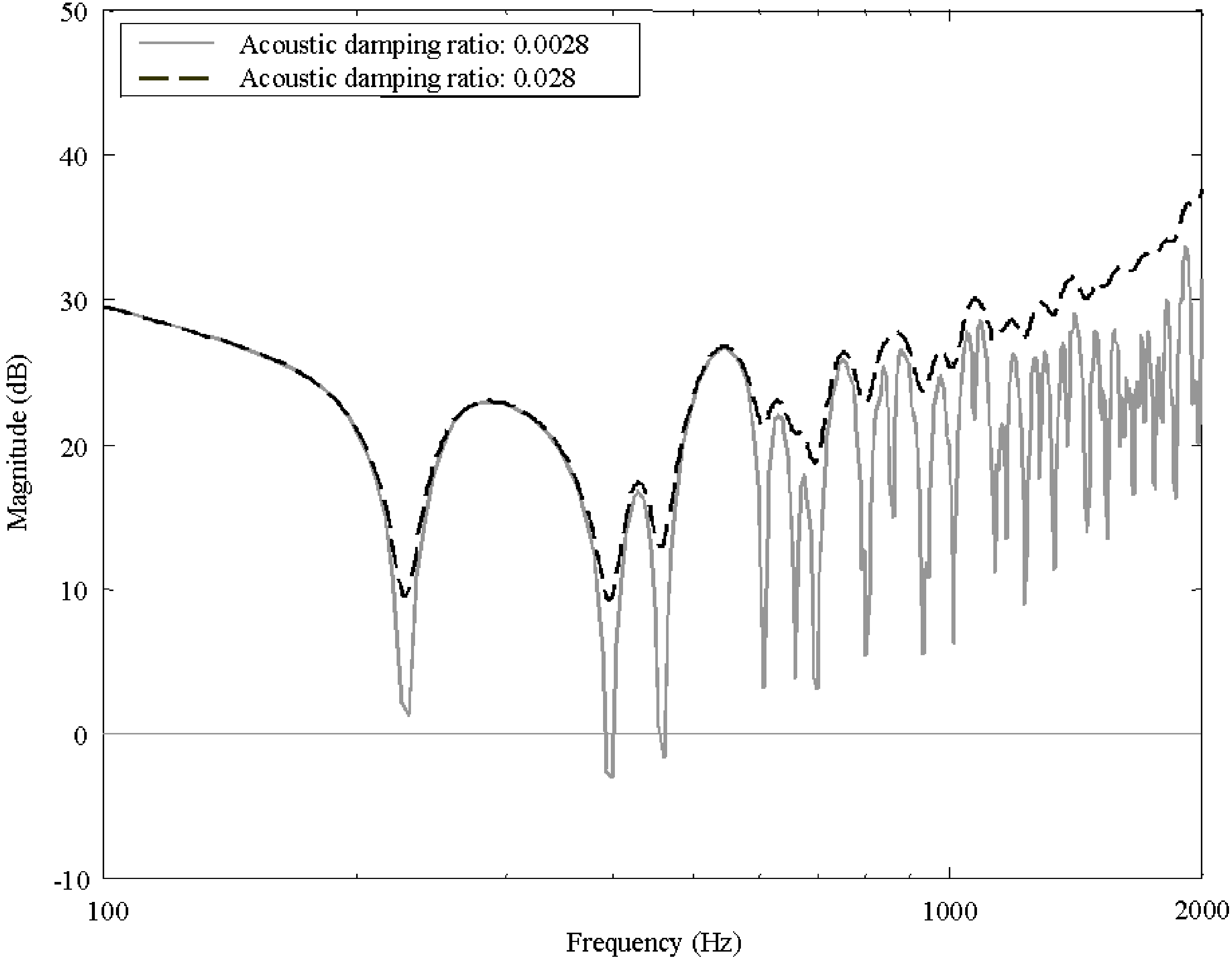
Acoustic damping ratio: 0.0028
Acoustic damping ratio: 0.028
Magnitude (dB)
Frequency (Hz)
50
40
30
20
10
0
-10
100
1000
2000

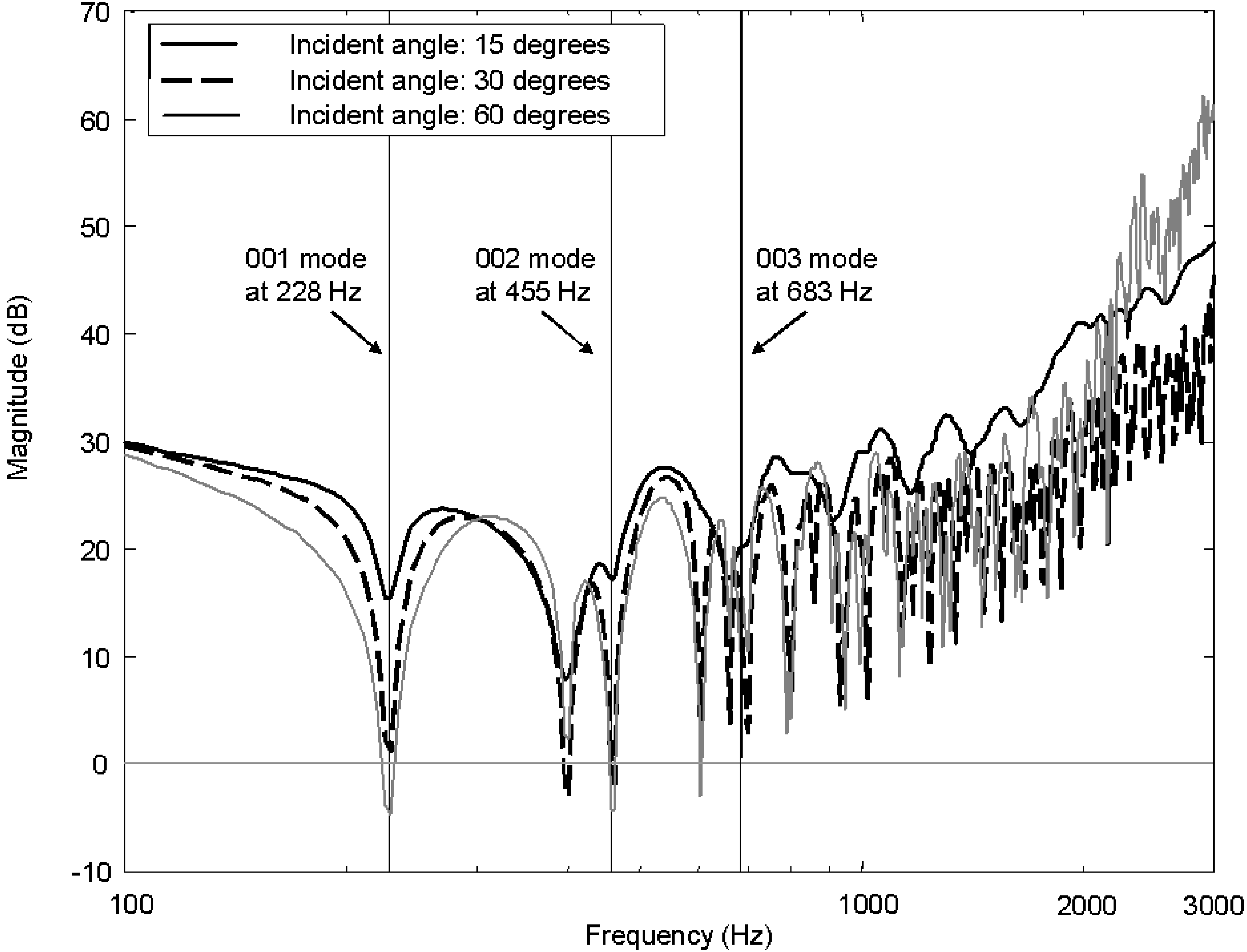

Incident angle: 15 degrees
Incident angle: 30 degrees
Incident angle: 60 degrees
001 mode
at 228 Hz
002 mode
at 455 Hz
003 mode
at 683 Hz
Magnitude (dB)
Frequency (Hz)
70
60
50
40
30
20
10
0
-10
100
1000
2000
3000

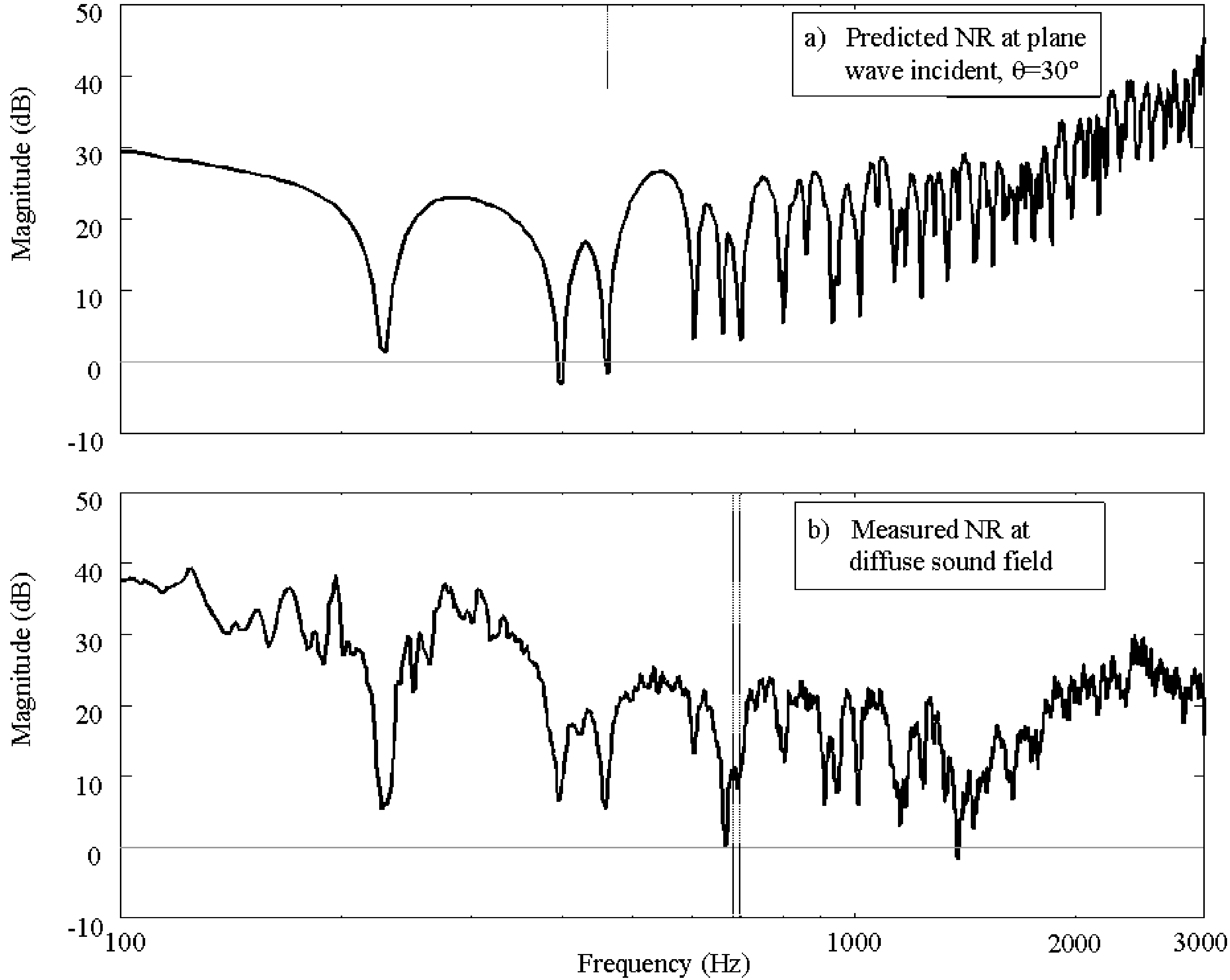
a) Predicted NR at plane wave incident, θ=30°
b) Measured NR at diffuse sound field
Magnitude (dB)
Magnitude (dB)
Frequency (Hz)
50
40
30
20
10
0
-10
100
1000
2000
3000